Stem Cell Reports
Report
ISSCR
OPEN ACCESS

Intrauterine Bone Marrow Transplantation in Osteogenesis Imperfecta Mice Yields Donor Osteoclasts and Osteomacs but Not Osteoblasts

Susan M. Millard,[1,2,*] Allison R. Pettit,[1,2] Rebecca Ellis,[1] Jerry K.Y. Chan,[1,3,4] Liza J. Raggatt,[1,2] Kiarash Khosrotehrani,[1,5] and Nicholas M. Fisk[1,6]

[1]UQ Centre for Clinical Research, The University of Queensland, Herston, QLD 4029, Australia
[2]Mater Research Institute, The University of Queensland, Translational Research Institute, Woolloongabba, QLD 4102, Australia
[3]Department of Reproductive Medicine, KK Women's and Children's Hospital, Singapore 229899, Singapore
[4]Experimental Fetal Medicine Group, Department of Obstetrics and Gynaecology, National University of Singapore, Singapore 119228, Singapore
[5]UQ Diamantina Institute, The University of Queensland, Translational Research Institute, Woolloongabba, QLD 4102, Australia
[6]Royal Brisbane and Women's Hospital, Centre for Advanced Prenatal Care, Herston, QLD 4029, Australia
*Correspondence: susan.millard@mater.uq.edu.au
http://dx.doi.org/10.1016/j.stemcr.2015.09.017

INTRODUCTION

Osteogenesis imperfecta (OI) represents a spectrum of genetic disorders characterized by skeletal fragility and low-impact fractures. Severity ranges from modest fracture risk to extreme risk with intrauterine fractures and skeletal malformations. Heterogeneity results from variability in the range of causative mutations, with the vast majority directly affecting the principle protein component of bone, collagen type I, resulting in bone matrix of insufficient quantity and/or quality (Cundy, 2012). Bisphosphonates, anti-resorptive drugs that reduce bone turnover, are commonly prescribed in severe OI; while they increase bone mass, their efficacy in reducing fractures is less clear (Dwan et al., 2014; Palomo et al., 2015). Furthermore, their mode of action does not address the underlying cause of OI and is associated with undesirable skeletal side effects in children (Rauch et al., 2007).

Cell therapy has considerable potential in treating OI, as replacing abnormal osteoblasts, the bone-forming cells with defective bone matrix production, with normal functioning osteoblasts should improve both bone quality and quantity and mimic the naturally occurring mosaic mutation carriers who demonstrate normal skeletal health (Cabral and Marini, 2004). Thus, replacement of just 25% of osteoblasts may deliver significant benefit to OI patients. Small clinical trials and isolated case studies of cell therapy for severe OI have already been undertaken, with considerable variation in transplantation protocols and donor cell source. Growth velocity transiently improved in children with OI following both bone marrow transplantation and subsequent mesenchymal stromal/stem cell (MSC) transplantation (Horwitz et al., 1999, 2001, 2002). Clinical experience following in utero transplantation of fetal MSC is also consistent with modest transient benefit (Götherström et al., 2014; Le Blanc et al., 2005). Given the low-level donor chimerism reported, this cannot be conclusively attributed to donor osteopoiesis. These few case studies are also subject to confounding factors of bisphosphonate co-treatment and inherent phenotypic heterogeneity of OI. While promising, the potential of cell therapy has yet to be substantiated and is now more comprehensively addressed in preclinical studies.

Preclinical models allow assessment of cell therapy in larger sample sizes with more consistent disease presentation in the absence of confounding co-therapies. The key target for cell replacement is the osteoblast that produces the collagen type I bone matrix. As such, mesenchymal stromal/stem cells (MSCs) are an obvious cell therapy candidate, as they are believed to be the source of long-term osteoblast repopulation in vivo. However, a recent study on adolescent osteogenesis imperfecta (*oim/oim*) mice concluded non-adherent BM cells were superior to MSC at contributing to osteopoiesis (Otsuru et al., 2012). Furthermore, intra-uterine transplantation of murine whole BM in the Brtl IV mouse model of OI reduced perinatal lethality and was associated with improved bone biomechanics (Panaroni et al., 2009). However, the methods to quantitate chimerism were independent of rigorous confirmation of donor cells being osteoblasts. This is of particular concern following BM transplantation, where donor cells may contribute to hematopoietic-derived bone cells, including osteoclasts and osteal macrophages (Chang et al., 2008). Hence, the capacity of donor cells to contribute to osteopoiesis following bone marrow transplantation remains unclear. To address this, we profiled the identity of bone-associated donor cells following intra-uterine bone marrow transplantation in the *oim/oim* mouse.

RESULTS

Generation of *oim/oim* Mice with Chimeric Bone Marrow

Fetuses homozygous for a null mutation (*oim*) in the collagen type I alpha 2 gene (COL1A2) underwent intra-uterine bone marrow transplantation (BM-IUT) at e14.5,

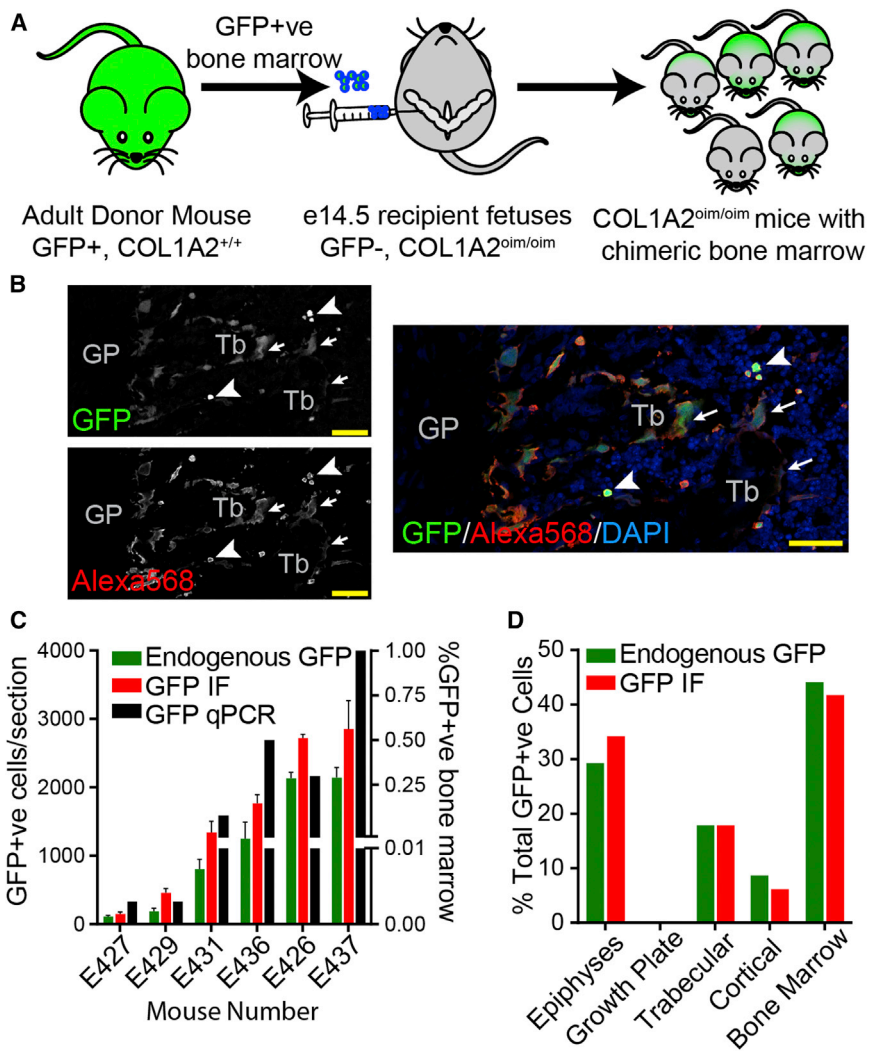

Figure 1. Generation of Osteogenesis Imperfecta Mice with Chimeric Bone Marrow

(A) Intrauterine transplantation of bone marrow from adult CAG-EGFP mice was performed on e14.5 *oim/oim* embryos, resulting in mice with low-level bone marrow chimerism.

(B) Longitudinal humeral cryosection of humerus displays strong correlation between endogenous GFP fluorescence and GFP immunostaining. Scale bar, 200 μm. GP, growth plate; Tb, trabecular bone. Arrowheads indicate GFP^+ cells in the bone marrow. Arrows indicate GFP^+ cells on the bone surface.

(C) Quantitation of chimerism in six individual 6-week-old mice by three methods—enumeration of cells with either endogenous GFP fluorescence or immunostaining for GFP (GFP IF) and quantitation of donor DNA in femoral bone marrow (GFP qPCR). Cell counts are means ±SD from at least three cryosections.

(D) Distribution of GFP^+ cells within different regions of interest, as indicated. Data shown for an individual mouse (E436) are typical.

receiving BM from GFP-expressing donors with wild-type COL1A2 alleles (Figure 1A). BM-IUT was performed in eight pregnant mice and control injections in three pregnant mice, resulting in 63 BM-IUT and 25 control *oim/oim* fetuses. Of these, 22 (35%) BM-IUT and 13 (52%) control neonates survived to P2, consistent with known fetal loss rates following murine IUT (Chan et al., 2007; Panaroni et al., 2009). Further losses occurred post-birth, consistent with our experience with breeding homozygous *oim/oim* without experimental intervention, such that 12 BM-IUT (19% of transplanted fetuses) and four controls (16%) survived postnatally to the experimental endpoint of 6 weeks.

Chimerism was first assessed by qPCR to detect GFP sequence in genomic DNA isolated from femoral BM. GFP sequence was amplified in eight of 12 BM-IUT mice (66%) but was not detectable in any controls. Of eight chimeric mice, chimerism was quantifiable in four (range: 0.08%–1%; Figure 1C) but was at the assay detection limit (0.003%) in the other four animals. The identity of chimeric animals was confirmed by immunofluorescent staining for GFP in humeral sections. Antibody-mediated staining co-localized with endogenous GFP fluorescence (Figure 1B) and increased sensitivity of donor cell detection by at least 30%. Enumeration of GFP^+ cells in humeri, identified by endogenous fluorescence (range: 116–2,146 GFP^+ cells/section), correlated with chimerism rates in femoral BM established by qPCR on gDNA (Figure 1C; Spearman ρ 0.93, $p < 0.02$). Donor cell distribution was assessed by dividing the humerus into five regions of interest: epiphyses (humeral head), growth plate (cartilage), trabecular bone surfaces (both primary and secondary spongiosa), diaphyseal cortical surfaces, and BM of medullar cavity. Donor cells were in all compartments except the cartilaginous growth plate (Figure 1D). Cells associated with bone surfaces (trabecular and cortical compartments, and a portion of the epiphyseal compartment) typically

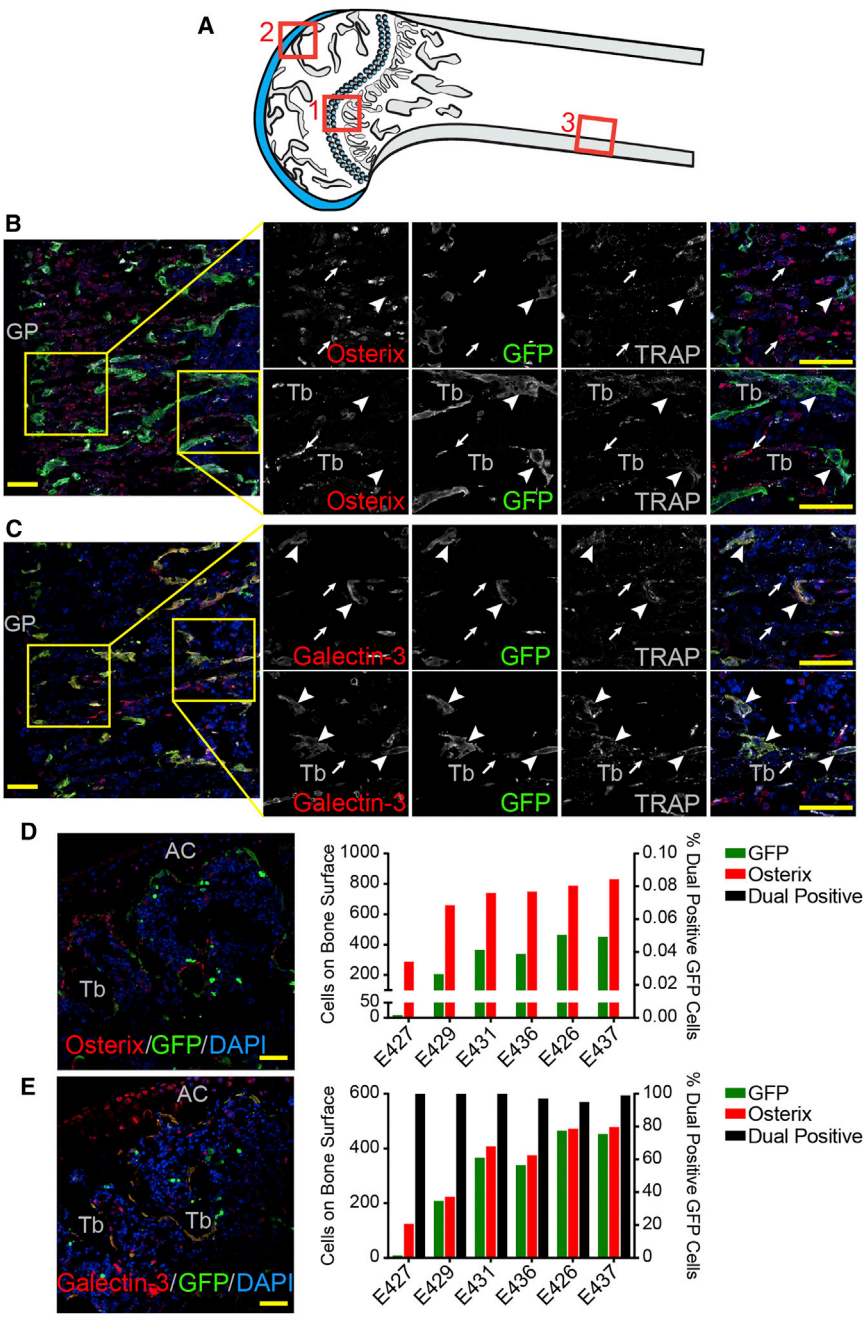

Figure 2. The Majority of Bone Surface-Associated Donor Cells Are Osteoclasts

(A) Representation of a longitudinal section of the humerus showing three regions of interest: (1) growth plate and primary spongiosa, (2) epiphyseal, and (3) endocortical.

(B and C) Images of region of interest 1 from humeral sections co-stained for donor cells (GFP), osteoclasts (TRAP), and either the osteoblast marker, osterix (B), or the osteoclast-expressed galectin-3 (C). Insets displayed at higher magnification show mineralized cartilage and primary spongiosa (upper panel) and maturing trabecular bone (lower panel). GP, growth plate. Arrowheads indicate cells with broad TRAP$^+$ staining. Arrows indicate cells with no TRAP$^+$ staining or punctate TRAP$^+$ staining consistent with osteoblastic endocytosis of TRAP from the bone surface.

(D and E) Co-staining for donor cells (GFP) and either osterix (D) or galectin-3 (E) within the epiphyses. Tb, trabecular bone; AC, articular cartilage. GFP$^+$ cells on the bone surface within the epiphyses were enumerated and the percentage of those also positive for either osterix (D) or galectin-3 (E) calculated. The average cell counts from two sections are displayed. Scale bars, 50 μm. See also Figure S1.

accounted for more than 20% of GFP$^+$ve donor cells enumerated within each humerus.

Bone-Associated Donor Cells Are Osteoclasts and Osteomacs, Not Osteoblasts

The identity of chimeric cells associated with the bone surface was examined by staining for osterix (early osteoblast lineage commitment marker), galectin-3 (abundantly expressed by osteoclasts and chondrocytes), and activity of Tartrate-Resistant Acid Phosphatase (TRAP; a classical marker for osteoclasts). The highest frequency of bone-associated donor cells was within trabecular bone of primary spongiosa (Figures 2B and 2C) and the epiphyses (Figures 2D and 2E). There was complete absence of co-expression of osterix and GFP, in contrast to almost complete overlap observed between GFP and galectin-3 staining on bone surfaces. Bone adjacent GFP$^+$/galectin-3$^+$ cells were also TRAP$^+$, confirming their osteoclast identity. Within non-bony regions (e.g., marrow, articular cartilage), there was no overlap between GFP and galectin-3 staining,

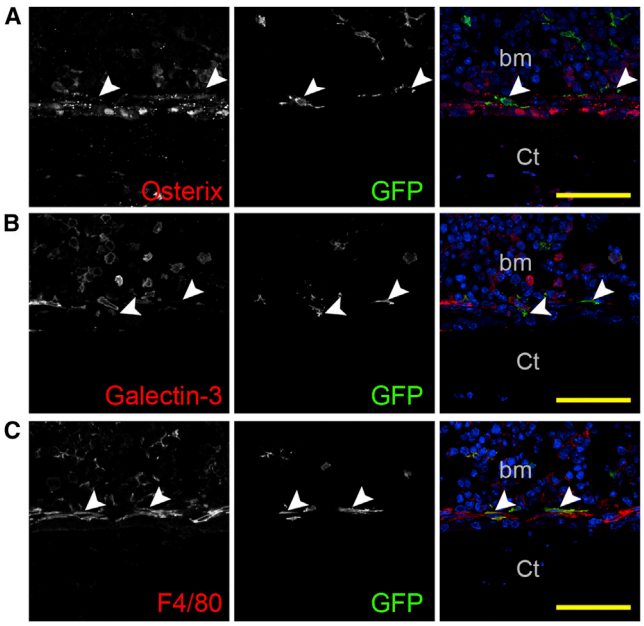

Figure 3. Some Endo-cortical-Associated Donor Cells Are F4/80$^+$ Osteal Macrophages

(A–C) Endo-cortical surface co-stained for donor cells (GFP) and either osterix (A), galectin-3 (B), or the macrophage marker F4/80 (C). bm, bone marrow; Ct, cortical bone. Scale bars, 50 μm. Arrowheads indicate the location of GFP$^+$ bone-associated donor cells that are osterix negative, galectin-3 negative, and F4/80$^+$.

nor did GFP$^+$ cells display TRAP$^+$ staining (Figure 2E; data not shown).

Histomorphometric analysis of the epiphysis revealed complete absence of co-staining of GFP and the early osteoblast marker, osterix, within the context of abundant single staining GFP$^+$ or osterix$^+$ cells on bone surfaces (Figure 2D). Furthermore, no co-staining of GFP and osterix was observed in any other region. Semiquantitative analysis indicated the average humeral section contained >2,800 osterix$^+$ cells (>700 in epiphysis, >1,000 primary spongiosa, ~100 secondary spongiosa, >1,000 on endocortical bone surfaces). If chimerism rates of 0.1%–1% were achieved in the osteoblast lineage, then five to 56 GFP$^+$ve cells would be expected within the >5,600 osterix$^+$ osteoblasts surveyed in each mouse, rather than the observed absence. Similarly, co-staining for GFP and either collagen type I or the mature osteoblast marker osteocalcin revealed complete absence of dual positive cells (Figure S1; data not shown). This indicates that donor cells did not contribute to osteoblast lineage cells after BM-IUT transplantation in *oim/oim* mice.

In contrast to the lack of donor-derived osteoblasts, there was a substantial contribution of donor cells to the osteoclast lineage. Galectin-3 staining was chosen as a surrogate osteoclast marker for two reasons: (1) the close correlation in bone-associated cells between galectin-3 expression and activity of the classical osteoclast marker, TRAP, and (2) the ability simultaneously to observe GFP and galectin-3 staining by epifluorescence microscopy. The proportion of GFP$^+$ cells on epiphyseal bone surfaces also galectin-3$^+$ ranged from 95%–100% (Figure 2E). Furthermore, except for instances where GFP$^+$ cell frequency was very low (≤0.003% BM), the proportion of galectin-3$^+$ osteoclasts that were GFP$^+$ ranged from 85%–95%, suggesting a preferential contribution of donor cells to the osteoclast lineage. This pattern of GFP and galectin-3 co-localization was also observed in primary spongiosa (Figure 2C) and on cortical surfaces. These data indicate that the vast majority of bone-associated donor cells following BM-IUT in *oim/oim* mice are osteoclasts.

Three of six mice had a notable fraction (1%–5%) of bone-associated donor cells that lacked galectin-3 expression. These were most marked in mouse E426 and readily detectable on endocortical surfaces. They lacked both osterix and galectin-3 expression and were located in close proximity to osterix$^+$ osteoblasts (Figure 3). Staining for the macrophage marker, F4/80, demonstrated these to be osteal macrophages, (Figure 3), bone regulatory cells of the hematopoietic lineage.

Spontaneous Fractures in Chimeric *oim/oim* Mice

Although lack of donor cell contribution to osteoblast lineage cells largely obviates the potential for improved bone matrix properties following BM-IUT, it does not exclude the possibility of phenotypic benefit by alternative mechanisms. The prevalence of spontaneous long bone fractures in 6-week-old chimeric BM-IUT *oim/oim* mice (median = 1 fracture/mouse; range = 0–4) is consistent with observations in *oim/oim* mice without intervention (Figure 4A; data not shown). Curiously, very few fractures were observed in the four control animals that had undergone intrauterine injection of PBS or the four BM-IUT animals in which no chimerism was observed (Figure 4A). In the chimeric BM-IUT mice, no correlation was observed between the frequency of donor chimerism and number of spontaneous fractures (Figure 4B). Donor-derived osteoclasts, but not donor-derived osteoblasts, were found within fracture sites (Figures 4C and 4D). These data suggest no phenotypic benefit from BM-IUT in *oim/oim* mice.

DISCUSSION

BM-IUT in *oim/oim* resulted in demonstrable hematopoietic chimerism in 66% of mice at 6.7 weeks post-transplantation, at levels of up to 1%. This is consistent with previous reports of hematopoietic chimerism following

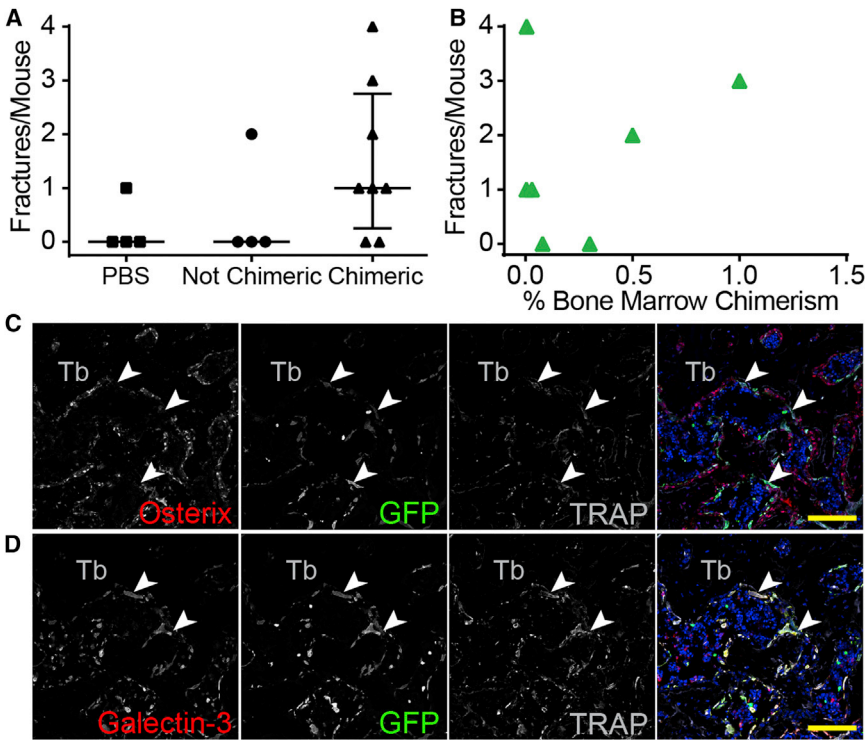

Figure 4. Donor Chimerism Did Not Prevent Fractures in Osteogenesis Imperfecta Mice, and Donor Cells Did Not Contribute to the Osteoblast Lineage within Fracture Sites

(A) Occurrence of spontaneous long bone fractures in 6-week-old mice.

(B) Fracture number plotted against chimerism rate determined by qPCR.

(C and D) Sections of fracture callus co-stained for donor cells (GFP), osteoclasts (TRAP), and either osterix (C) or galectin-3 (D). Tb, trabecular bone. Scale bars, 100 μm. Arrowheads indicate the location of some GFP$^+$ bone-associated donor cells.

BM-IUT into hematologically normal recipients (Panaroni et al., 2009). A competitive advantage of recipient fetal HSC over donor adult HSC in both replication rate and early occupation of stem cell niches likely contributes to these low levels of chimerism. Due to the hybrid strain background of the *oim/oim* mice, the H-2 haplotype of each recipient mouse may have been syngeneic (b), haploidentical (b/k), or allogeneic (k) with donor cells. Had all transplants been syngeneic, this may have increased the frequency of chimeric mice and the levels of chimerism observed. Hematopoietic micro-chimerism is not always associated with donor tolerance (Kim et al., 1998), and the frequency of chimeric recipients following allogeneic BM-IUT declines with time post-transplant (Peranteau et al., 2007). All chimeric mice displayed GFP$^+$ donor cells within the myeloid lineage (GFP$^+$/F4/80$^+$ macrophages), lymphoid lineage (based on morphological identification of GFP$^+$ lymphocytes—being small round and primarily consisting of nucleus), and robust numbers of bone-associated donor cells. We subsequently focused on the characterization of these bone-associated donor cells.

Bone-associated donor cells were primarily located in epiphyseal and metaphyseal regions where significant bone turnover is occurring in maturing 6-week-old mice. Despite the large numbers of bone-associated donor cells following BM-IUT (up to 1,300 per longitudinal humeral section), none expressed the osteoblast markers; osterix, collagen type I or osteocalcin. Furthermore, endocortical bone surface, with which donor cells showed the least association, was observed to be primarily lined by osteoblasts. Instead, bone-associated donor cells were identified as osteoclasts (TRAP$^+$; Galectin-3$^+$) or osteal macrophages (F4/80$^+$; TRAP$^-$) (Alexander et al., 2011). Our data document a complete absence of donor-derived osteopoeisis following BM-IUT in *oim/oim* mice and highlight the inadequacy of using only association with the bone-surface to assign osteoblastic identity to donor-derived cells.

The morphology and localization of bone-associated donor cells we describe is consistent with that seen following BM-IUT in the BrtlIV OI model (Panaroni et al., 2009) or bone marrow transplantation (BMT) in adolescent *oim/oim* mice (Otsuru et al., 2012). We postulate that bone-associated donor cells observed in the BrtlIV model may also be osteoclasts rather than osteoblasts (Panaroni et al., 2009), as the identity of these cells was not profiled. Colony-forming assays on recipient BM revealed donor-derived GFP$^+$ fibroblastic colony-forming units (CFU-F). However, multiple cell types contribute to CFU-F including macrophages (Xu et al., 1983), which are hematopoietic lineage cells. The identity of bone-associated donor cells following BMT in adolescent *oim/oim* is less clear (Otsuru et al., 2012). In this very different transplant paradigm involving recipient pre-conditioning with lethal irradiation, donor cells expressed wild-type collagen type I, but this alone is insufficient to assign osteoblastic identity. Macrophages can express collagen type I in certain

circumstances including wound healing (Vaage and Lindblad, 1990; Zreiqat et al., 2003). Further in a murine BM transplantation model, donor cells expressing GFP under control of a 3.6-kb fragment of the COL1A1 promoter were shown not to be functional osteoblasts (Wang et al., 2005). Within donor animals, these reporter-expressing cells were associated with active mineralization fronts and early osteoblasts. Following transplantation into irradiated recipient mice they were frequently associated with bone surfaces but never with active mineralization fronts, and they failed to progress to osteocytes. Consequently, we argue that there is currently no conclusive evidence for donor osteopoeisis following BMT in models of OI and that production of collagen by non-osteoblastic donor cells may contribute to the transient clinical benefit observed in patients following BM transplantation. In our model of BM-IUT without irradiation induced injury, we observed neither measurable phenotypic benefit nor collagen type I expression in donor-derived osteal macrophages.

While donor osteoblasts were absent following BM-IUT in *oim/oim* mice, there was a disproportionate contribution of donor cells to osteoclasts. Not only were 95%–100% of bone-associated donor cells identified as $TRAP^+$/Galectin-3^+ osteoclasts, but over 90% of osteoclasts were GFP^+. This was enumerated at the epiphyses, but was also apparent at the primary spongiosa and fracture sites. Osteoclasts are multi-nucleated cells formed by cell fusion, and a single GFP^+ pre-cursor would lead to a GFP^+ osteoclast. Variation in GFP expression levels by osteoclasts is suggestive of variation in the number of GFP^+ precursors contributing to each osteoclast. Nonetheless, the extent of GFP^+ osteoclasts (90% versus $\leq$1% assessed in qPCR of bone marrow) represents a lineage bias, the reason for which is unclear. While both osteoclasts and osteal macrophages, $F4/80^+$ which account for the galectin-3 negative bone-associated donor cells, are derived from myeloid precursors, over-representation of donor cells was not observed in osteal macrophages.

Consistent with the lack of donor osteopoeitic contribution, our data offer no support for donor chimerism reducing spontaneous fracture rate in *oim/oim* mice. As at other sites, donor cells within fractures were primarily osteoclasts, with an absence of donor-derived osteoblasts. Curiously, fracture occurrence in control groups appeared lower than expected. In our recent experience with untreated 6-week-old *oim/oim* mice ($n > 40$), the median number of long bone fractures is one per mouse, with 55% having at least one fracture at this age, whereas here long bone fractures were observed in just one in four mice for each control group; PBS injected IUT sham and non-chimeric transplant recipients. This may reflect selection bias toward more robust animals in the surviving analysis cohort, representing <20% of fetal PBS/BMT recipients. Survival rates of 10%–60%, dependent on mouse strain/disease model, are typical of murine IUT experiments (Chan et al., 2007; Panaroni et al., 2009). Hence, selection bias may provide an alternative explanation for the superior bone biomechanical properties observed in BM-IUT-treated BrtlIV mice compared with untreated (rather than sham-operated) controls (Panaroni et al., 2009). This emphasizes the importance of sham-operated controls in fetal and neonatal cell therapy experiments in OI models.

Previous evidence summarized above is insufficient to indicate that BM cells are superior to MSC at contributing to osteopoiesis in preclinical models of OI. We report a lack of donor osteopoeisis following BM-IUT in *oim/oim* mice, and posit that there is no adequate evidence to date that BM-IUT yields clinical benefit in treatment of OI. In the postnatal model of BMT following lethal irradiation, a population of collagen type I-expressing donor cells can be found on bone surfaces, with production of normal collagen matrix by such cells potentially contributing the transient benefit observed following BM transplants in OI children (Horwitz et al., 1999, 2001; Otsuru et al., 2012). However, without demonstrating that donor cells are true osteoblasts that contribute to mineralization, it seems improbable that BMT alone provides sustained clinical benefit in OI patients. Hence, we reiterate that MSC with their demonstrable osteogenic potential remain the obvious candidate for development of cell therapy for OI. Systemic transplantation of murine MSC in neonatal animals led to chimerism of up to 28% (Li et al., 2007), but this is atypical. Fetal and neonatal transplant recipients of human fetal MSC display <5% chimerism (Guillot et al., 2008; Li et al., 2007; Vanleene et al., 2011), with worse results observed in older animals receiving adult murine MSC (Otsuru et al., 2011; Pauley et al., 2014). Several studies have shown increased bone formation following local intra-femoral transplantation of murine MSC in *oim/oim* mice (Li et al., 2010; Pauley et al., 2014). Here, donor cells expressing a bone-specific reporter were localized to active mineralization fronts, thus demonstrating donor osteopoiesis. This activity was serially transplantable, indicating the persistence of an osteogenic stem cell/progenitor (Pauley et al., 2014). Such studies provide critical proof of principle of the capacity of transplanted MSC to contribute to osteopoeisis in an OI setting. However, local transplantation is not an ideal solution to a systemic skeletal disorder, and the local transplantation protocols tested in preclinical models involve onerous conditioning of recipients, such as sublethal irradiation or concurrent whole BM transplant. Successful development of cell therapy for OI requires improved understanding of how to create niches

for MSC engraftment in order to allow sustained donor chimerism.

EXPERIMENTAL PROCEDURES

Animals and Intrauterine Transplantation

Animals were used in accordance with the Australian Code of Practice for the Care and Use of Animals for Scientific Purposes and approved under institutional guidelines for humane use of animals in research. Osteogenesis imperfecta (*oim/oim*) mice and CAG-EGFP mice are described in the Supplemental Experimental Procedures. Fresh bone marrow was harvested from hind-limb long bones of 8- to 10-week-old CAG-EGFP mice, subjected to red blood cell lysis and resuspended in PBS supplemented with 2% fetal bovine serum (FBS). Following timed matings of *oim/oim* mice, pregnant dams underwent intrauterine transplantation at embryonic day 14.5, with each fetus receiving 5×10^6 CAG-EGFP nucleated bone marrow cells by intraperitoneal injection. Litters of control fetuses undergoing the same surgical procedure were injected with 10 μl PBS/2% FBS. Due to the hybrid strain background of *oim/oim* mice, the H-2 haplotype of recipient fetuses may be syngeneic (b), haploidentical (b/k), or allogeneic (k) with donor cells. Neonatal survival was assessed at P2, and mice were monitored until tissue harvest at 6 weeks of age.

Fracture Assessment

Whole skeletal imaging was conducted on isoflorane-anesthetized mice at 2, 4, and 6 weeks of age using the Kodak DXS 4000 Pro System with Carestream MI 5.0.6 software (Bruker). Images were obtained at an X-ray energy of 35 kVp, f-stop of 5.6- and 2.4-min exposure time. Fractures were scored in humeri, femurs, and tibia on the basis of a notable fracture callous or bone deformity.

gDNA Isolation and Assessment

Genomic DNA was isolated from bone marrow flushed from the right femur, using QIAamp DNA mini kit (QIAGEN). TaqMan qPCR assays determined the amount of donor specific gDNA sequence (GFP) relative to a murine reference sequence (ApoB). Bone marrow isolated from CAG-EGFP mice was used to generate standard curves for quantitation.

Tissue Sectioning and Fluorescent Staining

Fluorescent staining for tartrate-resistant acid phosphatase (TRAP) and immunofluorescent staining were conducted on longitudinal cryosections of non-decalcified humeri supported on Kawamoto cryofilm (Section Lab). Fluorescence images were captured by confocal microscopy. For further details and antibodies, see Supplemental Experimental Procedures.

Quantitative Analysis

Cryosections were visualized by epifluorescence microscopy using an EGFP/DsRed dual band excitation filter set on an AxioImager M1 (Zeiss). Sections were scanned using 40× objective, and the number of positive staining cells were enumerated at morphologically distinct regions of interest: epiphyses (bone marrow and bone surface), growth plate, trabecular bone (primary and secondary spongiosa), cortical bone, and bone marrow. For further details, see Supplemental Experimental Procedures.

SUPPLEMENTAL INFORMATION

Supplemental Information includes Supplemental Experimental Procedures and one figure and can be found with this article online at http://dx.doi.org/10.1016/j.stemcr.2015.09.017.

ACKNOWLEDGMENTS

Grant funding was provided by the National Health and Medical Research Council of Australia, Project ID: 631641.

Received: September 29, 2014
Revised: September 22, 2015
Accepted: September 22, 2015
Published: October 29, 2015

REFERENCES

Alexander, K.A., Chang, M.K., Maylin, E.R., Kohler, T., Müller, R., Wu, A.C., Van Rooijen, N., Sweet, M.J., Hume, D.A., Raggatt, L.J., and Pettit, A.R. (2011). Osteal macrophages promote in vivo intramembranous bone healing in a mouse tibial injury model. J. Bone Miner. Res. *26*, 1517–1532.

Cabral, W.A., and Marini, J.C. (2004). High proportion of mutant osteoblasts is compatible with normal skeletal function in mosaic carriers of osteogenesis imperfecta. Am. J. Hum. Genet. *74*, 752–760.

Chan, J., Waddington, S.N., O'Donoghue, K., Kurata, H., Guillot, P.V., Gotherstrom, C., Themis, M., Morgan, J.E., and Fisk, N.M. (2007). Widespread distribution and muscle differentiation of human fetal mesenchymal stem cells after intrauterine transplantation in dystrophic mdx mouse. Stem Cells *25*, 875–884.

Chang, M.K., Raggatt, L.J., Alexander, K.A., Kuliwaba, J.S., Fazzalari, N.L., Schroder, K., Maylin, E.R., Ripoll, V.M., Hume, D.A., and Pettit, A.R. (2008). Osteal tissue macrophages are intercalated throughout human and mouse bone lining tissues and regulate osteoblast function in vitro and in vivo. J. Immunol. *181*, 1232–1244.

Cundy, T. (2012). Recent advances in osteogenesis imperfecta. Calcif. Tissue Int. *90*, 439–449.

Dwan, K., Phillipi, C.A., Steiner, R.D., and Basel, D. (2014). Bisphosphonate therapy for osteogenesis imperfecta. Cochrane Database Syst. Rev. *7*, CD005088.

Götherström, C., Westgren, M., Shaw, S.W., Aström, E., Biswas, A., Byers, P.H., Mattar, C.N., Graham, G.E., Taslimi, J., Ewald, U., et al. (2014). Pre- and postnatal transplantation of fetal mesenchymal stem cells in osteogenesis imperfecta: a two-center experience. Stem Cells Transl. Med. *3*, 255–264.

Guillot, P.V., Abass, O., Bassett, J.H., Shefelbine, S.J., Bou-Gharios, G., Chan, J., Kurata, H., Williams, G.R., Polak, J., and Fisk, N.M. (2008). Intrauterine transplantation of human fetal mesenchymal stem cells from first-trimester blood repairs bone and reduces fractures in osteogenesis imperfecta mice. Blood *111*, 1717–1725.

Horwitz, E.M., Prockop, D.J., Fitzpatrick, L.A., Koo, W.W., Gordon, P.L., Neel, M., Sussman, M., Orchard, P., Marx, J.C., Pyeritz, R.E., and Brenner, M.K. (1999). Transplantability and therapeutic effects of bone marrow-derived mesenchymal cells in children with osteogenesis imperfecta. Nat. Med. *5*, 309–313.

Horwitz, E.M., Prockop, D.J., Gordon, P.L., Koo, W.W., Fitzpatrick, L.A., Neel, M.D., McCarville, M.E., Orchard, P.J., Pyeritz, R.E., and Brenner, M.K. (2001). Clinical responses to bone marrow transplantation in children with severe osteogenesis imperfecta. Blood *97*, 1227–1231.

Horwitz, E.M., Gordon, P.L., Koo, W.K., Marx, J.C., Neel, M.D., McNall, R.Y., Muul, L., and Hofmann, T. (2002). Isolated allogeneic bone marrow-derived mesenchymal cells engraft and stimulate growth in children with osteogenesis imperfecta: Implications for cell therapy of bone. Proc. Natl. Acad. Sci. USA *99*, 8932–8937.

Kim, H.B., Shaaban, A.F., Yang, E.Y., Liechty, K.W., and Flake, A.W. (1998). Microchimerism and tolerance after in utero bone marrow transplantation in mice. J. Surg. Res. *77*, 1–5.

Le Blanc, K., Götherström, C., Ringdén, O., Hassan, M., McMahon, R., Horwitz, E., Anneren, G., Axelsson, O., Nunn, J., Ewald, U., et al. (2005). Fetal mesenchymal stem-cell engraftment in bone after in utero transplantation in a patient with severe osteogenesis imperfecta. Transplantation *79*, 1607–1614.

Li, F., Wang, X., and Niyibizi, C. (2007). Distribution of single-cell expanded marrow derived progenitors in a developing mouse model of osteogenesis imperfecta following systemic transplantation. Stem Cells *25*, 3183–3193.

Li, F., Wang, X., and Niyibizi, C. (2010). Bone marrow stromal cells contribute to bone formation following infusion into femoral cavities of a mouse model of osteogenesis imperfecta. Bone *47*, 546–555.

Otsuru, S., Rasini, V., Bussolari, R., Hofmann, T.J., Dominici, M., and Horwitz, E.M. (2011). Cytokine-induced osteopoietic differentiation of transplanted marrow cells. Blood *118*, 2358–2361.

Otsuru, S., Gordon, P.L., Shimono, K., Jethva, R., Marino, R., Phillips, C.L., Hofmann, T.J., Veronesi, E., Dominici, M., Iwamoto, M., and Horwitz, E.M. (2012). Transplanted bone marrow mononuclear cells and MSCs impart clinical benefit to children with osteogenesis imperfecta through different mechanisms. Blood *120*, 1933–1941.

Palomo, T., Fassier, F., Ouellet, J., Sato, A., Montpetit, K., Glorieux, F.H., and Rauch, F. (2015). Intravenous bisphosphonate therapy of young children with osteogenesis imperfecta: skeletal findings during follow up throughout the growing years. J. Bone Miner. Res. Published online June 8, 2015. http://dx.doi.org/10.1002/jbmr.2567.

Panaroni, C., Gioia, R., Lupi, A., Besio, R., Goldstein, S.A., Kreider, J., Leikin, S., Vera, J.C., Mertz, E.L., Perilli, E., et al. (2009). In utero transplantation of adult bone marrow decreases perinatal lethality and rescues the bone phenotype in the knockin murine model for classical, dominant osteogenesis imperfecta. Blood *114*, 459–468.

Pauley, P., Matthews, B.G., Wang, L., Dyment, N.A., Matic, I., Rowe, D.W., and Kalajzic, I. (2014). Local transplantation is an effective method for cell delivery in the osteogenesis imperfecta murine model. Int. Orthop. *38*, 1955–1962.

Peranteau, W.H., Endo, M., Adibe, O.O., and Flake, A.W. (2007). Evidence for an immune barrier after in utero hematopoietic-cell transplantation. Blood *109*, 1331–1333.

Rauch, F., Cornibert, S., Cheung, M., and Glorieux, F.H. (2007). Long-bone changes after pamidronate discontinuation in children and adolescents with osteogenesis imperfecta. Bone *40*, 821–827.

Vaage, J., and Lindblad, W.J. (1990). Production of collagen type I by mouse peritoneal macrophages. J. Leukoc. Biol. *48*, 274–280.

Vanleene, M., Saldanha, Z., Cloyd, K.L., Jell, G., Bou-Gharios, G., Bassett, J.H., Williams, G.R., Fisk, N.M., Oyen, M.L., Stevens, M.M., et al. (2011). Transplantation of human fetal blood stem cells in the osteogenesis imperfecta mouse leads to improvement in multiscale tissue properties. Blood *117*, 1053–1060.

Wang, L., Liu, Y., Kalajzic, Z., Jiang, X., and Rowe, D.W. (2005). Heterogeneity of engrafted bone-lining cells after systemic and local transplantation. Blood *106*, 3650–3657.

Xu, C.X., Hendry, J.H., Testa, N.G., and Allen, T.D. (1983). Stromal colonies from mouse marrow: characterization of cell types, optimization of plating efficiency and its effect on radiosensitivity. J. Cell Sci. *61*, 453–466.

Zreiqat, H., Kumar, R.K., Markovic, B., Zicat, B., and Howlett, C.R. (2003). Macrophages at the skeletal tissue-device interface of loosened prosthetic devices express bone-related genes and their products. J. Biomed. Mater. Res. A *65*, 109–117.